# Increased Mitochondrial Dysfunction Associated with Autophagy and Mitophagy in Cerebrospinal Fluid Cells Following Subarachnoid Hemorrhage in Patients with Delayed Cerebral Ischemia

**Dong Hyuk Youn**
Hallym University College of Medicine
**Youngmi Kim**
Hallym University College of Medicine
**Bong Jun Kim**
Hallym University College of Medicine
**Myeong Seon Jeong**
Korea Basic Science Institute
**Jooeun Lee**
Korea Basic Science Institute
**Jong Kook Rhim**
Jeju National University College of Medicine
**Heung Cheol Kim**
Hallym University College of Medicine
**Jin Pyeong Jeon** ( jjs6553@daum.net )
Hallym University College of Medicine

**Research Article**

**Keywords:** Subarachnoid hemorrhage, autophagy, delayed cerebral ischemia, cerebrospinal fluid

**Posted Date:** April 9th, 2021

**DOI:** https://doi.org/10.21203/rs.3.rs-394833/v1



**Version of Record:** A version of this preprint was published at Scientific Reports on August 13th, 2021.
See the published version at https://doi.org/10.1038/s41598-021-96092-2.

# Abstract

Decreased mitochondrial membrane potential in cerebrospinal fluid (CSF) was observed in patients with subarachnoid hemorrhage (SAH) accompanied with delayed cerebral ischemia (DCI); however, the underlying mechanism remains unclear. We evaluated the mitochondrial dysfunction associated with autophagy and mitophagy in CSF cells for possible insight into DCI pathogenesis. CSF samples were collected from 56 SAH patients (DCI, n=21; and non-DCI, n=35). We analyzed CSF cells using autophagy and mitophagy markers (DAPK1, BNIP3L, BAX, PINK1, ULK1, and NDP52) via qRT-PCR and western blotting of proteins (BECN1, LC3, and p62). Confocal microscopy and immunogold staining were performed to demonstrate the differentially expression of markers within dysfunctional mitochondria. Significant induction of autophagic flux with accumulation of autophagic vacuoles, increased expression of BECN1, LC3-II, and p62 degradation were observed during DCI. DCI patients showed a significantly increased mRNA expression (2-ΔCt) than non-DCI patients: DAPK1, 0.279 (0.220–0.297) in DCI vs. 0.043 (0.021–0.086) in non-DCI; BNIP3L, 0.134 (0.060–0.202) in DCI vs. 0.045 (0.020–0.101) in non-DCI; and PINK1, 0.064 (0.044–0.810) in DCI vs. 0.045 (0.012–0.063) in non-DCI. Other markers including BAX, ULK1, and NDP52 did not differ significantly. The vWF-positive CSF cells showed a colocalization with antibodies for DAPK1, BNIP3L/NIX, PINK1, and BECN1 with dysfunctional mitochondria. Increased dysfunctional mitochondria associated with autophagy and mitophagy are closely associated with DCI pathogenesis.


# Introduction

Subarachnoid hemorrhage (SAH) is defined as acute bleeding in the subarachnoid space due to ruptured intracranial aneurysm. Despite advances in minimally invasive surgery, the mortality rates in patients presenting with poor-grade SAH remains high: 24% for Hunt and Hess (H-H) grade 4 and 71% for grade 5.[1] Medical complications following SAH are still a challenge in neurocritical care, even if ruptured aneurysm is treated successfully. Among the complications, early brain injury (EBI) and delayed cerebral ischemia (DCI) are major contributors to poor neurologic outcomes in patients with SAH. The clinical syndrome of DCI is characterized by newly developed neurologic deficits with symptom fluctuation, and usually occurs between 4 and 14 days after SAH ictus.[2,3] DCI pathogenesis is known to be associated with cerebral vasospasm, cortical spreading depolarization, and microthrombosis or EBI. However, the mechanisms underlying DCI have yet to be elucidated.

Autophagy is a reparative process in which cellular homeostasis is maintained through the lysosomal degradation of dysfunctional cytoplasmic components.[4] In particular, when healthy mitochondria are maintained though the selective removal of damaged or dysfunctional mitochondria via autophagy, this is referred to as mitophagy.[5,6] For SAH, the process was mainly focused on brain injury in the early stage after SAH, not the DCI. Lee at al.[5] reported a higher expression of beclin-1 (BECN1), microtubule-associated protein light chain-3 (LC3) conversion, and cathepsin-D in the frontobasal cortex, suggesting increased autophagy in neurons following SAH. Zhang et al.[7] also showed that mitophagy was

associated with oxidative stress-related neuronal death in rat SAH models induced by endovascular perforation. Recently, Youn et al.[8] showed significantly decreased mitochondria membrane potential in the cerebrospinal fluid (CSF) mitochondria on day 5 in SAH patients with DCI than in those without DCI. Under cerebral ischemic conditions, mitochondrial depolarization leads to the increased synthesis of reactive oxygen species (ROS), PTEN-induced kinase 1 (PINK1), and elevated unfolded protein response.[9,10] Considering the facts mentioned, we hypothesized that mitochondrial dysfunction associated with autophagy and mitophagy in CSF cells may be associated with DCI pathogenesis following SAH.

# Results

# Clinical outcomes

A total of 56 SAH patients treated with endovascular coil embolization were included in the analysis (Table 1). Twenty-one (37.5%) patients experienced DCI during the follow-up. The Cohen's kappa score for DCI diagnosis was 0.889, indicating almost perfect agreement (Supplemental Data). There was no statistical difference in clinical findings (e.g., female gender, age, hypertension, diabetes mellitus, hyperlipidemia and smoking status) between the two groups. SAH patients with DCI tended to exhibit higher Hunt and Hess grades of ≥ IV, but the difference was not statistically significant. The number of anterior circulation aneurysms in DCI and non-DCI patients were 17 (81.0%) and 28 (80.0%), respectively.

**Table 1**

Comparison of baseline characteristics of the study.

| Variables | Non-DCI (n=35) | DCI (n=21) | p-value |
|---|---|---|---|
| **Clinical findings** | | | |
| Female | 22 (62.9%) | 17 (81.0%) | 0.154 |
| Age, years | 62.7 ± 17.1 | 57.5 ± 10.5 | 0.157 |
| Hypertension | 18 (51.4%) | 9 (42.9%) | 0.534 |
| Diabetes mellitus | 4 (11.4%) | 2 (9.5%) | 0.823 |
| Hyperlipidemia | 4 (11.4%) | 4 (19.0%) | 0.430 |
| Smoking | 4 (11.4%) | 3 (14.3%) | 0.754 |
| Hunt and Hess grade ≥ IV | 11 (31.4%) | 11 (52.4%) | 0.120 |
| **Laboratory findings** | | | |
| Hemoglobin | 11.6 ± 1.2 | 12.0 ± 1.2 | 0.849 |
| $SaO_2$ (%) | 94.9 ± 1.6 | 95.3 ± 1.5 | 0.369 |
| Heart rate (BPM) | 89.6 ± 8.0 | 90.5 ± 7.2 | 0.664 |
| **Radiologic findings** | | | |
| Size (mm) | 5.3 ± 1.3 | 5.7 ± 0.9 | 0.225 |
| Anterior circulation | 28 (80.0%) | 17 (81.0%) | 0.931 |

BPM, beats per minute; DCI, delayed cerebral ischemia.

[a] Data are shown as the numbers of subjects (percentage) for discrete and categorical variables, and mean ± standard deviation.

# Morphological changes in mitochondria of SAH patients with DCI

Transmission electron microscopy (TEM) was used to investigate the changes in subcellular ultrastructure of CSF cells obtained from SAH patients with DCI (Figure 1). Numerous autophagic vacuoles containing mitochondria and fusion of autophagic vacuoles with abnormal mitochondria with swollen matrix and collapsed cristae accumulated in CSF cells. Additional autophagic vacuoles appeared close to the swollen mitochondria with inner mitochondrial membrane, indicating that the mitochondrial dysfunction with morphological impairment was associated with autophagic flux, and suggesting the possibility of autophagy and mitophagy in CSF cells in DCI pathogenesis.

# Increased autophagy in mitochondria of CSF cells

The mRNA of autophagy and mitophagy markers in CSF cells was measured and compared between SAH patients with and without DCI. Real-time quantitative PCR (qRT-PCR) was performed for all enrolled patients. DCI patients exhibited significantly higher expression ($2^{-\Delta Ct}$) than non-DCI patients: death-associated protein kinase (DAPK)-1, 0.279 (0.220–0.297) in DCI vs. 0.043 (0.021–0.086) in non-DCI, p<0.0001; BCL2 interacting protein 3 like (BNIP3L), 0.134 (0.060–0.202) in DCI vs. 0.045 (0.020–0.101) in non-DCI, p=0.0008; and PINK1, 0.064 (0.044–0.810) in DCI vs. 0.045 (0.012–0.063) in non-DCI, p=0.009. Other mRNAs expressed such as Bcl-1 antagonist X (BAX), 0.204 (0.167–0.294) in DCI vs. 0.166 (0.095–0.223) in non-DCI, p=0.178; Unc-51 like autophagy activating kinase 1 (ULK1), 0.013 (0.003–0.027) in DCI vs. 0.004 (0.001–0.008) in non-DCI, p=0.070; and nuclear dot protein 52 (NDP52), 0.258 (0.045–0.323) in DCI vs. 0.155 (0.030–0.229) in non-DCI, p=0.143 (Figure 2A). We further analyzed autophagy markers including ULK1, BECN, LC3, and p62 in CSF cells of DCI (n=6) vs. non-DCI patients (n=6). Western blot revealed increased protein expression of BECN1 and its phosphorylation at Ser15 in DCI patients compared with non-DCI patients (Figures 2B, 2C, and Supplemental Table S2). In addition, increased LC3II expression and p62 degradation were also observed in DCI patients. Mitochondria dysfunction-related proteins (BNIP3L/NIX, DAPK1, and PINK1) were enhanced in the CSF cells obtained from DCI patients.

# Autophagy and mitophagy in vWF-positive CSF cells in DCI

Previously, we demonstrated that cells of endothelial origin, shown as von Willebrand factor (vWF)-positive, were increasingly detected in the CSF of DCI patients concomitant with decreased mitochondria membrane potential.[8] To investigate whether mitochondrial dysfunction with increased autophagy and mitophagy occurred in vWF-positive CSF cells in SAH patients with DCI, multi-colored immunofluorescence staining was conducted with antibodies specific for vWF and MTDR as a marker of dysfunctional mitochondria (Figure 3). The fluorescence signals of DAPK1, BNIP3L/NIX, PINK1, and BECN1 overlapped with that of Mito Tracker Deep Red (MTDR) in vWF-positive CSF cells. vWF-positive cells (green) were not stained with CD41 (platelet marker). The results suggested that increased mitochondrial dysfunction with autophagy and mitophagy in vWF-positive CSF cells are associated with DCI pathogenesis in SAH patients.

# Mitochondrial dysfunction concomitant with increased DAPK1 in DCI

We further performed immunogold labeling with anti-DAPK1 to confirm the subcellular localization of enhanced DPAK1 in CSF cells obtained from SAH patients with DCI (Figure 4). Interestingly, DAPK immunogold particles were mainly observed in damaged mitochondria with abnormal morphology, which is consistent with results presented in Figure 3. Taken together, these results suggest that increased DAPK1 may play a pivotal role in mitochondrial dysfunction during the development of DCI.

# Discussion

The clinical significance of mitochondrial dysfunction has not been well studied in the DCI following SAH. In the event of cerebral ischemia, mitochondria are damaged through a series of following steps: 1) depolarization of mitochondrial membrane potential; 2) PINK2 accumulation with decreased adenosine triphosphate (ATP) reduction; 3) abnormal mitochondrial fission and fusion; and 4) broken cellular homeostasis due to increased ROS and matric calcium and subsequent cell death.[9]Autophagy and mitophagy are induced to remove damaged mitochondria after ischemic insult, but the process can make it worse as well as the neuroprotective effect ultimately.[9] Baek et al.[11] reported that attenuated autophagic signaling by carnosine, an endogenous pleiotropic peptide, was associated with improvement of mitochondrial function against ischemic brain injury. On the other hand, BNIP3L causes excessive mitophagy leading to delayed neuronal loss.[12] Chen et al.[13] reported that -(-) Epigallocatechin-3-Gallate (EGCG) administration was beneficial for maintain autophagy flux by regulating Beclin-1 and LC3B. EGCG decreased oxyhemoglobin-induced mitochondrial dysfunction with decreased ROS production following SAH. Cao et al.[14] also reported that melatonin lessened mitophagy-associated NLRP3 inflammasome for EBI after SAH. Nonetheless, the therapeutic role of mitophagy in the DCI is still unknown. Compared with EBI, which occurs in the brain parenchyma in the first 72 h after SAH onset, DCI usually develops 3 days thereafter and peaks from days 7 to 14. SAH literally refers to acute hemorrhage within the subarachnoid space surrounding the cerebral arteries. Free hemoglobin within the subarachnoid space triggers oxidative stress and inflammation, resulting in DCI.[15] Chou et al.[16] initially investigated the functional relevance of mitochondria in human CSF samples following SAH. In their study, higher mitochondrial membrane potential reflected favorable functional outcomes during the 3-month follow-up. In particular, the higher percentage of mitochondria potentially originating in astrocytes was associated with a favorable outcome. In this study, we further evaluated autophagy and mitophagy markers in the CSF cells to reveal the underlying DCI pathogenesis based on mitochondrial dysfunction. Our study showed that increased mitochondrial dysfunction associated with autophagy and mitophagy in CSF cells may drive DCI pathogenesis. Among the markers, the DAPK1 expression varied most significantly between the DCI and non-DCI patients.

DAPK1 acts as a sensor of mitochondrial membrane potential in mitochondrial toxin-induced cell death.[17] Mitochondrial toxins, such as rotenone, and carbonyl cyanide m-chlorophenylhydrazone (CCCP), which is an uncoupler of mitochondrial oxidative phosphorylation induce loss of membrane potential and mitochondrial swelling leading to cell death via DAPK1 activation in neuroblastoma cells. In damaged mitochondria, the accumulation of PINK1 and LC3 on the outer membrane is accompanied by loss of membrane potential.[18] Stroke-induced neuronal cell death is related to DAPK1 signaling mediated via DAPK1-N-methyl-D-aspartate receptors (NMDARs), DAPK1-p53 and DAPK1-Tau in cerebral ischemia.[19] Tu et al.[20] reported that DAPK1 directly binds with NR2B subunit of NMDARs in the cortex of mice, leading to aggravation of calcium reflux by enhancing the NR1/NR2B channel conductance. In their study, the genetic deletion of DPAPK1 or administration of $NR2B_{CT}$, defined as carboxyl tail region consisting of amino acids 1292-1304, inhibited calcium reflux and protected neuronal injury against ischemic

insults.[19, 20] DAPK-1 was also involved in the regulation of inflammation. Activation of DAPK led to decreased T cell activation and IL-2 production.[21,22] Chuang et al.[22] reported that DAPK was a regulator of T cell receptor (TCR)-activated NF-kappa B and T lymphocyte activation. Therefore, a further study elucidating the role of DAPK1 and T cell immunity in DCI pathogenesis in the CSF space is required.

In this study, we further evaluated the role of confocal microscopy to confirm the differential expression of autophagy and mitophagy markers in vWF positive-CSF cells of SAH patients with DCI.[16] The findings demonstrated colocalization with DAPK1, BNIP3L, PINK1, and BECN1-positive autophagosomes in mitochondria, suggesting mitochondrial dysfunction with autophagy and mitophagy in DCI pathogenesis. Endothelial dysfunction is related to cerebrovascular disease. Nitric oxide and endothelin released from endothelium regulates vascular function.[23] Compared with healthy controls, SAH patients exhibit elevated synthesis of endothelial microparticles.[24] In addition, increased levels of CSF and plasma endothelin were observed in SAH patients with vasospasm.[23] In DCI patients, a higher percentage of vWF-positive mitochondria was observed compared with non-DCI patients.[8] Accordingly, future studies should focus on the alleviation of the mitochondrial dysfunction in CSF cells of endothelial origin in DCI patients.

This study has some limitations. First, we enrolled SAH patients treated with coil embolization, but not surgical clipping. The penetration of laminar terminalis or brain retraction injury during the clipping can contaminate the CSF component, and therefore, bias the results of CSF mitochondria. Therefore, we excluded them from our analysis. Second, no medical treatment or additional chemical angioplasty for DCI severity was considered in the interpretation of results. In general, suppression of autophagy contributes to increased cell death, but can lead to cytotoxicity under some circumstances.[25] Accordingly, studies investigating the role of autophagy and mitophagy in CSF cells are further required under various SAH conditions. Third, the results of the multivariate analysis to find risk factors for DCI including autophagy and mitophagy markers were not provided in our study. We performed multivariate analysis, but the appropriate odds ratio were not calculated due to the diverse autophagy and mitophagy markers, and the relative small number of the patients. In addition, mitochondria dysfunction is likely to vary depending on the initial SAH severity and thus may be associated with the patient's outcome. Although there was no statistical significance of autophagy and mitophagy markers according to the SAH severity and patient's outcome (Supplemental Table S3 and S4), multivariate analysis should be performed in consideration of various variables including autophagy and mitophagy markers in the large number of the SAH patients. Nevertheless, our study represents the first investigation of mitochondrial dysfunction associated with autophagy and mitophagy in CSF cells derived from SAH patients with DCI.

# Conclusions

Dysfunctional mitochondria with autophagy and mitophagy are closely associated with DCI pathogenesis in SAH patients.

# Materials And Methods

# Study population

The derivation cohort was derived from the regional stroke database between March 2016 and May 2020. We selected SAH patients from this database based on the following inclusion criteria: 1) adult patients > 18 years old; 2) SAH due to ruptured aneurysm; 3) dense localized clot and/or vertical layer of blood greater than 1mm in thickness on computed tomography (CT); and 4) SAH patients who were treated with endovascular coil embolization. The exclusion criteria were: 1) non-aneurysmal SAH such as trauma, infection or perimesencephalic SAH, 2) patients treated with surgical clipping and 3) previous history of central nervous system disorder or mitochondrial diseases.

TEM was used to detect the autophagic vacuoles and morphological changes of mitochondria in CSF cells derived from SAH patients with DCI. We evaluated and compared the autophagy and mitophagy biomarkers in CSF cells of SAH patients with and without DCI using qRT-PCR. The markers included DAPK-1, BNIP3L, BAX, PINK1, ULK1 and NDP52. We further evaluated the expression of autophagy executor gene of BECN1 and autophagy adaptor protein of p62.[26, 27] Confocal microscopy was used to identify colocalization of differentially expressed genes in vWF-positive CSF cells, which represented endothelial cell origin, and were increased in SAH patients with DCI.[8]

In our study, the diagnosis of DCI wad performed through the following criteria: 1) new developed neurological changes such as motor weakness, dysphasia, and sensory change; 2) decrease consciousness by more than 2 points via the Glasgow Coma Scale score or National Institutes of Health stroke scale; 3) fluctuation of symptoms lasing more than 1 hr; 4) cerebral infarction identified on CT or MRI, but not complications related to the endovascular coil embolization; 5) concomitant severe cerebral vasospasm with narrowing more than 50% compared to the initial radiological tests; and 6) excluding other causes that may neurological

changes such as re-bleeding, hydrocephalus, seizures or electrolyte imbalances.[2,28] DCI was monitored daily based on the transcranial Doppler (TCD) velocity. When severe vasospasm was suspected based on a TCD greater than 200 cm/s in the middle cerebral artery or 85 cm/s in the basilar artery,[29] catheter angiography was additionally performed to confirm the degree of vasospasm and chemical angioplasty, as needed. Poor outcome was defined by a modified Rankin scale (mRS) score of $\geq 3$ or Glasgow Outcome Scale (GOS) of $\leq 4$ at the 3-month follow-up.

After coil embolization, continuous lumbar drainage of CSF was maintained in the neurointensive care unit in every SAH patient for 1 week after ictus in our institution. Because difference in mitochondrial membrane potential of the CSF cells was most prominent on day 5 post ictus in SAH patients with and without DCI,[8] we analyzed the CSF samples obtained from days 5 to 7. Clinical, laboratory, and radiological information was reviewed by the two investigator independently. Disagreements were resolved by the third investigator. The protocol of DCI diagnosis among reviewers are presented in detail in the Supplemental Data. Sample collection and study design were performed according to the principles of the Declaration of Helsinki and were approved by the Institutional Review Board of the Chuncheon

Sacred Heart Hospital (No. 2017-9, 2018-6, and 2019-6). All methods were performed in accordance with the relevant guidelines and regulations in manuscript. Informed consent was received from the patients or their relatives.

# Transmission electron microscopy

Previously, SAH patients with DCI showed depolarization of mitochondrial membrane potential, which triggers alteration in mitochondrial function and morphologies.[8] In the present study, TEM was used to investigate the changes in subcellular ultrastructure of CSF cells in SAH patients with DCI. CSF samples were centrifuged at 4000 rpm for 10 min, and the pellets were analyzed by electron microscopy.[8] The pellets were fixed overnight in 2% glutaraldehyde in cacodylate buffer (0.1 M sodium cacodylate, 2 mM MgCl2) at 4 ℃. After washing three times with cacodylate buffer at 4℃, the samples were post-fixed in 2 % osmium tetroxide for 1 h at 4℃. The samples were rinsed with deionized water and dehydrated through a gradient series of ethanol, ranging from 50% to 100% ethanol, 20 min each step. The samples were incubated with progressively concentrated propylene oxide dissolved in ethanol followed by infiltration with increasing concentration of Eponate 812 resin. Samples were baked in a 65°C oven overnight and sectioned using an Ultra microtome. Sections were viewed with a Field Emission TEM unit (JEM-2100F, JEOL) at the Korean Basic Science Institute, Chuncheon, South Korea.[8]

# Western blot analysis

CSF cells obtained from SAH patients were lysed with RIPA buffer (50 mM Tris-base, 10 mM EDTA, 150 nM NaCl, 0.1 % SDS, 1 % Triton X-100, 1 % sodium deoxycholate, 1 mM PMSF). Protein lysates of the supernatant were quantified using the BCA protein assay kit (Thermo Scientific, USA). Equal amounts of protein were separated on 10 % SDS-polyacrylamide gel electrophoresis (SDS-PAGE) and transferred to PVDF membranes (Bio-Rad, USA). After blocking the membranes with 2 % BSA in TBS-T (Tris-buffered saline including 0.1 % Tween-20) for 1 h, the membranes were incubated with the primary antibodies overnight at 4℃. After extensive washing, the membranes were incubated with HRP-conjugated secondary antibodies, and developed using an enhanced chemiluminescence (ECL) kit (Thermo Scientific, USA). Antibodies used in this study were: BECN1 (#3495, Cell Signaling Technology, USA, dilution 1:1000), p62 (sc-48402, Santa Cruz Biotechnology, USA, dilution 1:1000), LC3 (#3868, Cell Signaling Technology, USA, dilution 1:1000), pBECN1Ser15 (#84966, Cell Signaling Technology, USA, dilution 1:1000), DAPK (PA5-14044, Invitrogen, USA, dilution 1:1000), PINK1 (ab23707, Abcam, UK, dilution 1;1000), BNIP3L/NIX (ab8399, Abcam, UK, dilution 1:1000), and actin (sc-47778, Santa Cruz Biotechnology, USA, dilution 1:1000)

# Immunofluorescence staining

To evaluate the colocalization of autophagy and mitophagy markers with dysfunctional mitochondria in vWF-positive CSF cells, multi-color immunofluorescence staining was performed via confocal microscopy. CSF cells were fixed with paraformaldehyde (4 % w/v) and then washed with PBS. After blocking with 2.5% blocking solution (Vector, USA) for 1h, the cells were incubated with antibodies specific to DAPK1 (PA5-14044, Invitrogen, USA, dilution 1:100), PINK1 (ab23707, Abcam, UK, dilution 1;100), BECN1 (#3495, Cell Signaling, USA, dilution 1;100) and BNIP3L/NIX (ab8399, Abcam, UK, dilution 1:100) overnight at 4℃. After incubation with anti-rabbit Alexa Fluor 750-conjugated secondary antibody (ab175733, Abcam, UK, dilution 1:500), the coverslips were mounted in Fluoroshield™ with DABCO (ImmunoBioScience Corp. USA). vWF-FITC (von Willebrand factor–fluorescein; ab8822, Abcam, UK, dilution 1:500, Abcam) was used as an endothelial marker to confirm the endothelial origin of CSF cells.[16] CD41 (GTX113758, GeneTex, USA, dilution 1:100) was used to differentiate endothelial and platelet, and it was confirmed that vWF was an endothelial specific marker in our study. To assess the dysfunctional mitochondria undergoing autophagy in vWF-positive CSF cells, autophagy- or mitophagy-related markers were subjected to co-immunofluorescence stained with MTDR (M22426, Invitrogen, USA, dilution 200 nM), which is widely used as a mitochondria-selective dye to determine mitophagy.[30] Nuclei were counterstained with 4',6-diamidino-2-phenylindole dihydrochloride (DAPI, D1306, Invitrogen, USA, dilution 300 nM). Fluorescence images were obtained via confocal microscopy at 400x magnification.

# Real time qRT-PCR

The loss of mitochondrial membrane potential leading to mitochondrial dysfunction results in activation of mitochondrial autophagy. Therefore, autophagy and mitophagy markers such as DAPK1, PINK1, BAX, BNIP3L, and NDP52 were examined in CSF cells.[17,18] Total RNAs were isolated from the CSF cells using TriZOL (Ivitrogen, USA) according to the manufacturer's instructions. The cDNA was synthesized from 5 μg of RNA using Maxime RT PreMix Kit (iNtRON Biotechnology, Korea). The expression of mitophagy-related genes was measured by qRT-PCR using the 2x Rotor-Gene SYBR Green PCR Master Mix (Qiagen, Carlsbad, CA, USA) in the Rotor-Gene Q (Qiagen, USA). Primer sequences are presented in the Supplemental Table S1.

# Immunogold staining

We further performed immunogold staining to confirm the location of the most significant differentially expressed markers within the mitochondria of CSF cells in SAH patients with DCI. CSF cells were fixed with 0.1% glutaraldehyde and 2% paraformaldehyde in phosphate buffer at pH 7.4 for 1 h at 4°C, followed by incubation with post-fixed osmium tetroxide for 30 min at 4°C. The samples were dehydrated in a graded series of ethanol. The samples were treated with graded ethanol series and embedded in LR white resin (EMS). The sections were then sliced into ultra-thin sections of 80 nm each, and placed on a copper grid. The sections were treated with 0.02 M glycine for 10 min to ensure quench-free aldehyde groups. Sections were then washed with deionized water, blocked in 1% BSA and incubated with rabbit

anti-DAPK1 antibodies (PA5-14044, Invitrogen, USA, dilution 1:100) for 1 h. The grid was washed five times with 0.1% BSA in PBS, and incubated with a secondary antibody conjugated with 10 nm gold (AUR810.011, AURION, Netherlands, dilution 1:100) in 0.1% BSA in PBS. The final samples were stained with uranyl acetate and lead citrate, and then visualized under a transmission electron microscope (JEOL-2100F, USA) at 200 KV.

# Statistical analysis

Continuous variables are expressed as the mean and ± standard deviation (SD). A chi-square or Student's t test was carried out to identify meaningful differences between DCI and non-DCI patients. Comparative analysis via qRT-PCR was performed using the Mann-Whitney U test. The results were presented as the median and $25^{th}$ -$75^{th}$ percentiles. Quantification of western blots using the relative optical densities with actin protein as the reference and presented as the mean ± standard error of the mean (SEM). Statistical analysis was performed with SPSS V.21 (SPSS, Illinois, USA) and GraphPad Prism software (v.6.01; GraphPad Software Inc., San Diego, CA, USA) with a statistical significance indicated at $p < 0.05$.

## Declarations

# Author contributions

JPJ designed and obtained funding for the study. DHY, BJK, YK, MSJ and JL were responsible for the molecular experiments. YK and JPJ interpreted the data and performed statistical analyses. JPJ provided input for the final version of the manuscript. All authors reviewed the manuscript and provided editorial feedback.

# Conflicts of interest

All authors declare no competing interests.

# Compliance with ethical standards

Sample collection and study design were performed according to the principles of the Declaration of Helsinki and were approved by Coordinating Ethnics Committee of the Chuncheon Sacred Heart Hospital.

# Data availability

Data are available from the corresponding author (JPJ) upon ethical approval from the IRB of the participating hospital.

# Acknowledgements

None

# Source of Funding

This research was supported by the National Research Foundation of Korea funded by the Ministry of Education (2020R1I1A3070726).

## References

1. Lantigua, H. et al. Subarachnoid hemorrhage: Who dies, and why? *Crit Care*. 19, 309 (2015).
2. Vergouwen, M.D. et al. Definition of delayed cerebral ischemia after aneurysmal subarachnoid hemorrhage as an outcome event in clinical trials and observational studies: Proposal of a multidisciplinary research group. *Stroke*. 41, 2391-2395 (2010).
3. Rowland, M.J. et al. Delayed cerebral ischaemia after subarachnoid haemorrhage: Looking beyond vasospasm. *Br J Anaesth*. 109, 315-329 (2012).
4. Ho, W.M. et al. Autophagy after subarachnoid hemorrhage: Can cell death be good? *Curr Neuropharmacol*. 16,1314-1319 (2018).
5. Lee, J.Y. et al. Activated autophagy pathway in experimental subarachnoid hemorrhage. *Brain Res*. 1287, 126-135 (2009).
6. Wu, W. et al. Pink1-parkin-mediated mitophagy protects mitochondrial integrity and prevents metabolic stress-induced endothelial injury. *PLoS One*. 10, e0132499 (2015).
7. Zhang, T. et al. Mitophagy reduces oxidative stress via keap1 (kelch-like epichlorohydrin-associated protein 1)/nrf2 (nuclear factor-e2-related factor 2)/phb2 (prohibitin 2) pathway after subarachnoid hemorrhage in rats. *Stroke*. 50, 978-988 (2019).
8. Youn, D.H., Kim, B.J., Kim, Y., Jeon, J.P. Extracellular mitochondrial dysfunction in cerebrospinal fluid of patients with delayed cerebral ischemia after aneurysmal subarachnoid hemorrhage. *Neurocrit Care*. 33, 422-428 (2020).
9. Liu, F. et al. Mitochondria in ischemic stroke: New insight and implications. *Aging Dis*. 9, 924-937 (2018).
10. Galluzzi, L., Kepp, O., Kroemer, G. Mitochondria: Master regulators of danger signalling. *Nat Rev Mol Cell Biol*. 13, 780-788 (2012).
11. Baek, S.H. et al. Modulation of mitochondrial function and autophagy mediates carnosine neuroprotection against ischemic brain damage. *Stroke*. 45, 2438-2443 (2014).
12. Shi, R.Y. et al. Bnip3 interacting with lc3 triggers excessive mitophagy in delayed neuronal death in stroke. *CNS Neurosci Ther*. 20, 1045-1055 (2014).

13. Chen, Y. et al. Reduction in autophagy by (-)-epigallocatechin-3-gallate (egcg): A potential mechanism of prevention of mitochondrial dysfunction after subarachnoid hemorrhage. *Mol Neurobiol*. 54, 392-405 (2017).
14. Cao, S. et al. Melatonin-mediated mitophagy protects against early brain injury after subarachnoid hemorrhage through inhibition of nlrp3 inflammasome activation. *Sci Rep*. 7, 2417 (2017).
15. Leclerc, J.L. et al. Haptoglobin phenotype predicts the development of focal and global cerebral vasospasm and may influence outcomes after aneurysmal subarachnoid hemorrhage. *Proc Natl Acad Sci U S A*. 112, 1155-1160 (2015).
16. Chou, S.H. et al. Extracellular mitochondria in cerebrospinal fluid and neurological recovery after subarachnoid hemorrhage. *Stroke*. 48, 2231-2237 (2017).
17. Shang, T., Joseph, J., Hillard, C.J., Kalyanaraman, B. Death-associated protein kinase as a sensor of mitochondrial membrane potential: Role of lysosome in mitochondrial toxin-induced cell death. *J Biol Chem*. 280, 34644-34653 (2005).
18. Wang, Y., Liu, N., Lu, B. Mechanisms and roles of mitophagy in neurodegenerative diseases. *CNS Neurosci Ther*. 25, 859-875 (2019).
19. Wang, S. et al. Dapk1 signaling pathways in stroke: From mechanisms to therapies. *Mol Neurobiol*. 54, 4716-4722 (2017).
20. Tu, W. et al. Dapk1 interaction with nmda receptor nr2b subunits mediates brain damage in stroke. *Cell*. 140, 222-234 (2010).
21. Lai, M.Z., Chen, R. H. Regulation of inflammation by dapk. *Apoptosis*. 19, 357-363 (2014).
22. Chuang, Y.T. et al. The tumor suppressor death-associated protein kinase targets to tcr-stimulated nf-kappa b activation. *J Immunol*. 180, 3238-3249 (2008).
23. Masaki, T., Sawamura, T. Endothelin and endothelial dysfunction. *Proc Jpn Acad Ser B Phys Biol Sci*. 82, 17-24 (2006).
24. Lackner, P. et al. Cellular microparticles as a marker for cerebral vasospasm in spontaneous subarachnoid hemorrhage. *Stroke*. 41, 2353-2357 (2010).
25. Zhang, J. Autophagy and mitophagy in cellular damage control. *Redox Biol*. 1, 19-23 (2013).
26. Seto, S., Tsujimura, K., Horii, T., Koide, Y. Autophagy adaptor protein p62/sqstm1 and autophagy-related gene atg5 mediate autophagosome formation in response to mycobacterium tuberculosis infection in dendritic cells. *PLoS One*. 8, e86017 (2013).
27. Comincini, S. et al. Identification of autophagy-related genes and their regulatory mirnas associated with celiac disease in children. *Int J Mol Sci*. 18 (2017).
28. Okazaki, T., Kuroda, Y. Aneurysmal subarachnoid hemorrhage: Intensive care for improving neurological outcome. *J Intensive Care*. 6, 28 (2018).
29. Samagh, N., Bhagat, H., Jangra, K. Monitoring cerebral vasospasm: How much can we rely on transcranial doppler. *J Anaesthesiol Clin Pharmacol*. 35, 12-18 (2019).

30. Mauro-Lizcano, M. et al. New method to assess mitophagy flux by flow cytometry. *Autophagy*. 11, 833-843 (2015).

# Figures

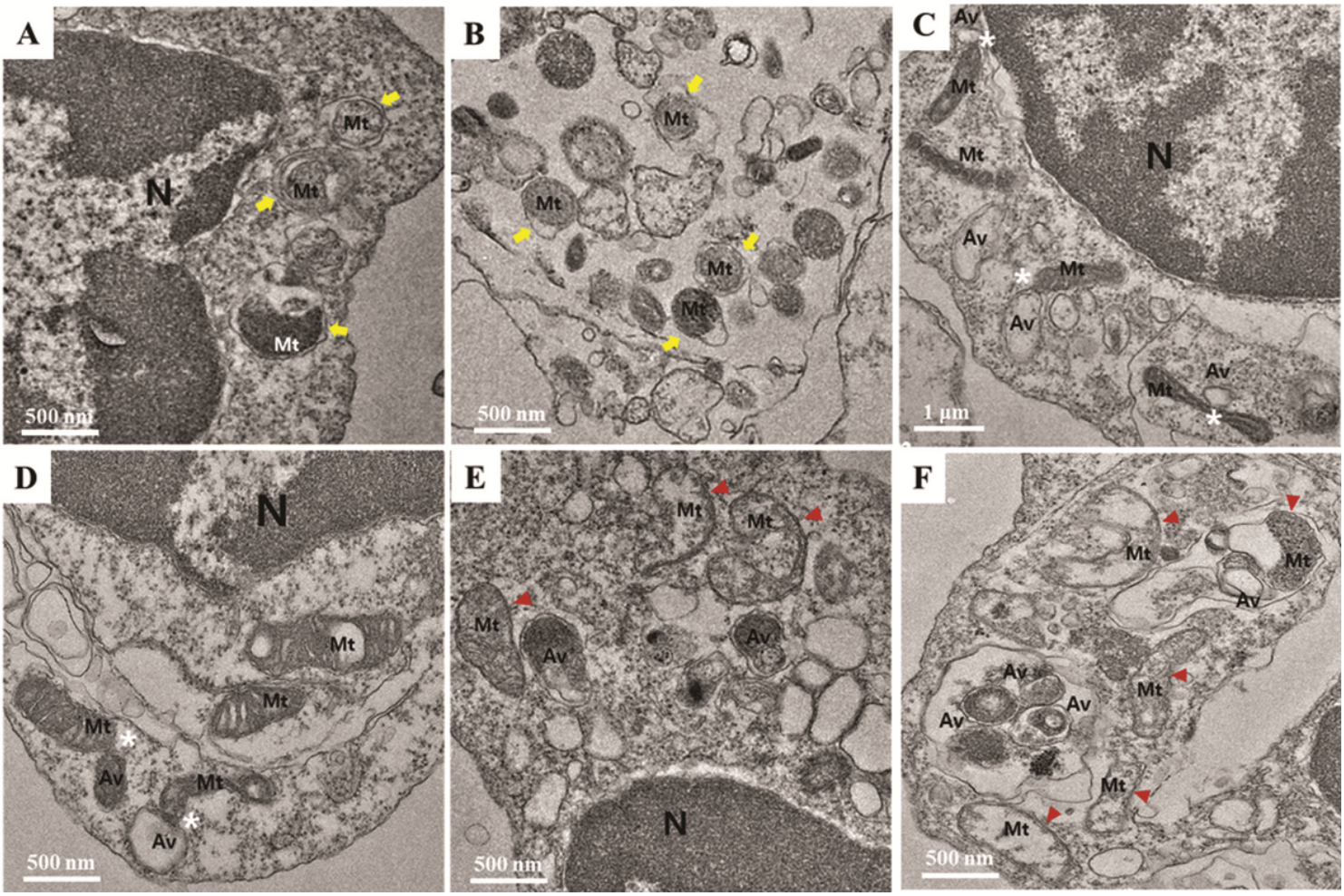


## Figure 1

Transmission electron microscopy images of mitochondrial dysfunction with autophagy and mitophagy in CSF cells from SAH patients with DCI. (A) and (B) Autophagic vacuoles containing damaged mitochondria are indicated with yellow arrows. (C) and (D) Interaction between mitochondria and autophagic vacuoles is indicated by white asterisks. (E) and (F) Autophagic vacuoles were observed close to damaged mitochondria (red arrowhead) with matrix swelling and collapsed cristae. Mt, mitochondria; Av, autophagic vacuoles; N, nuclear. Scale bar; 1 μm, 500 nm.

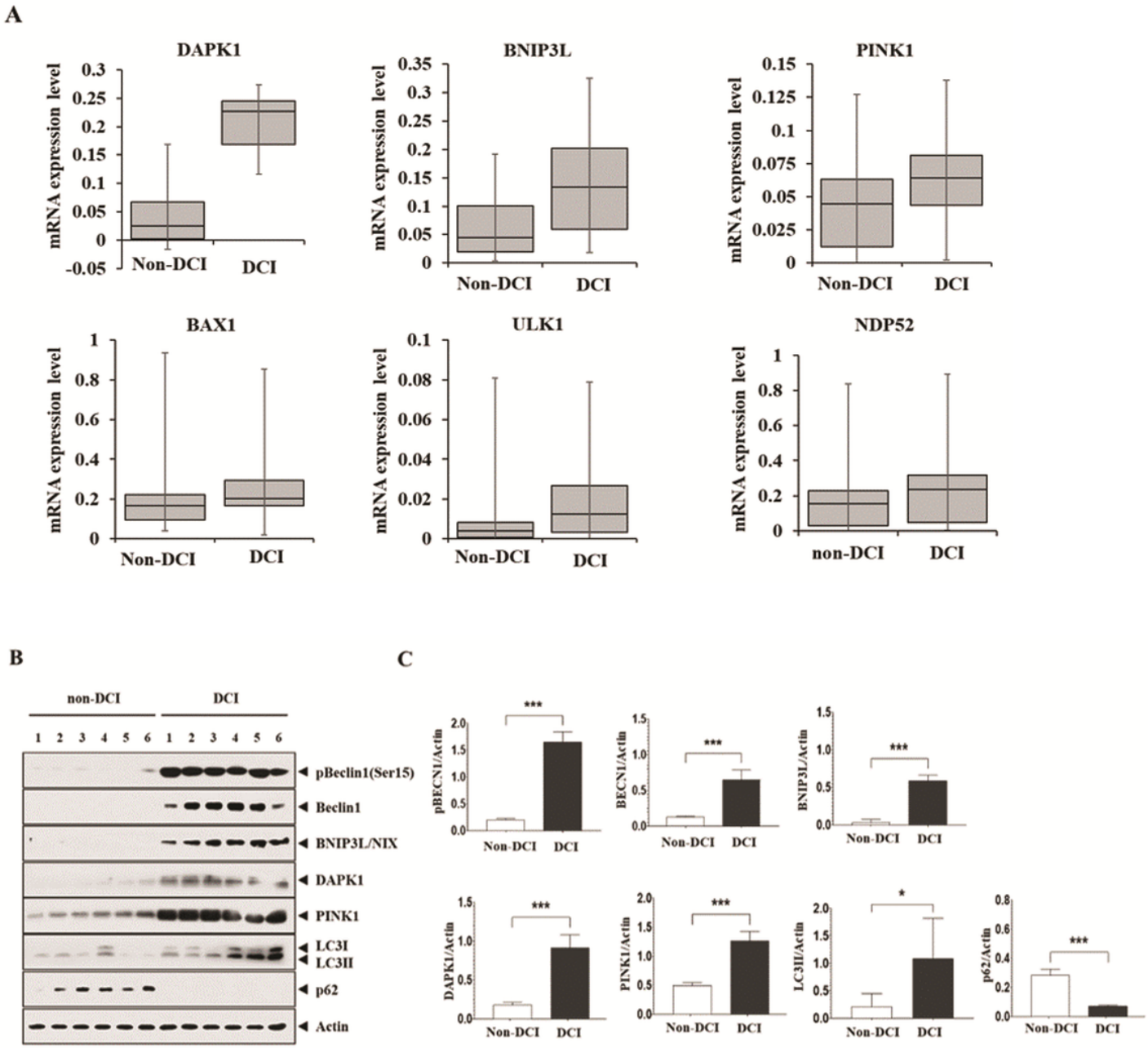


## Figure 2

Analysis of autophagy and mitophagy markers expressed in CSF cells of SAH patients. (A) qRT-PCR revealed that SAH patients with DCI exhibited increased mRNA expression of DAPK1, BNIP3L, and PINK1 compared with those without DCI. Differences in mRNA expression of BAX, ULK1, and NDP52 did not reach statistical significance between the two groups. (B and C) Western blot analysis and quantification of blots using relative optical densities. Increased expression of BECN protein and phosphorylation at Ser15. LC3II expression with p62 degradation was observed in SAH patients with DCI. Actin was used as the loading control. The error bars represent SEM. *, **, and *** represent p-value of less than of <0.05, 0.01, and 0.001, respectively.

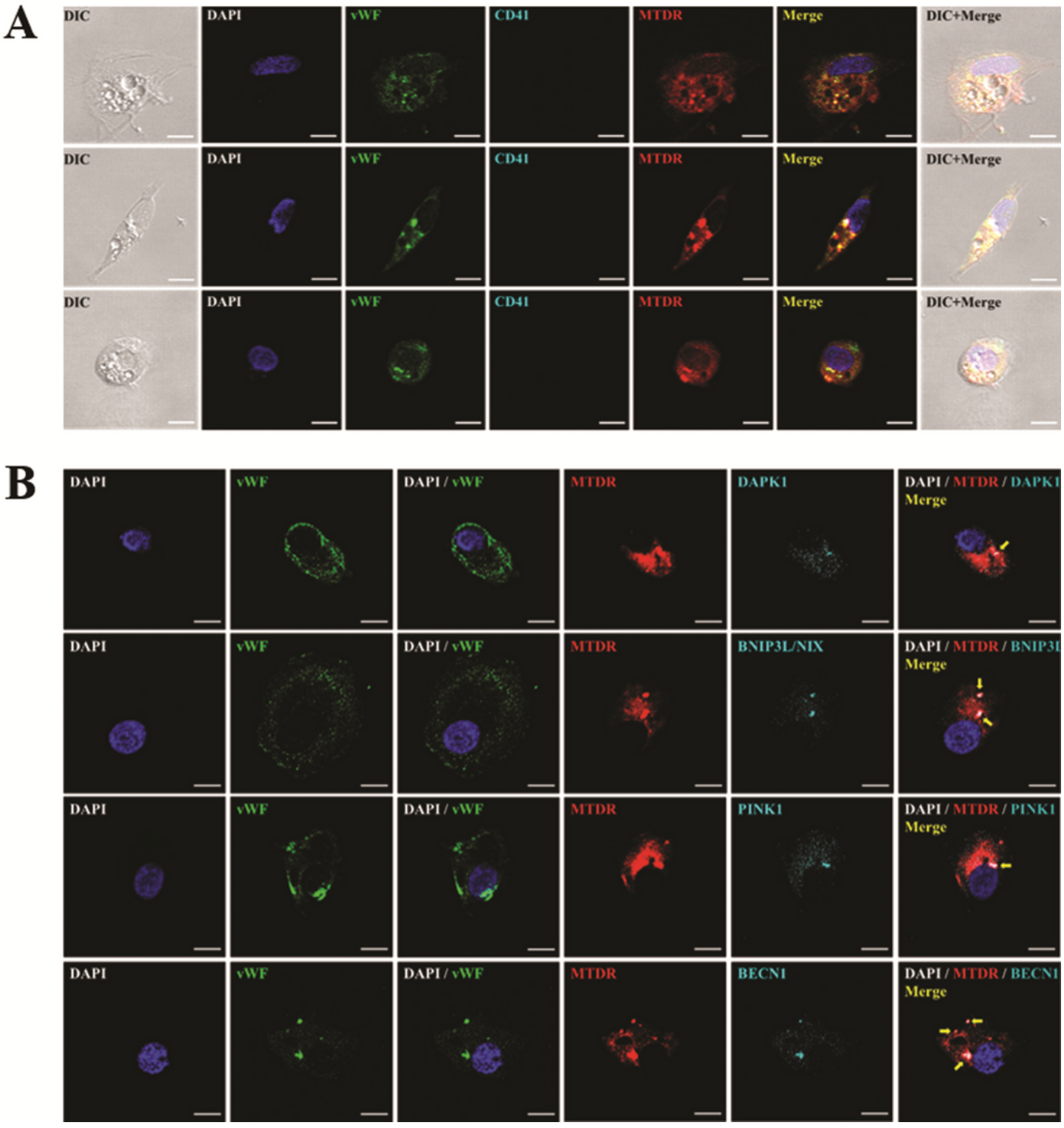


## Figure 3

Confocal microscopy of mitochondrial dysfunction with increased autophagy and mitophagy in CSF cells from SAH patients with DCI. (A) CSF cells were stained with DAPI, vWF, CD41, and MTDR. Columns 1, 6, and 7 show differential interference contrast (DIC) images, merged images, and DIC with merged images, respectively. (B) vWF-positive CSF cells were immunostained with antibodies specific for DAPK1, BNIP3L/NIX, PINK1, and BECN1, and analyzed microscopically. White dots indicated by yellow arrows

represent colocalization with autophagy and mitophagy markers in dysfunctional mitochondria under red fluorescence labeling. Scale bar, 20 μm.

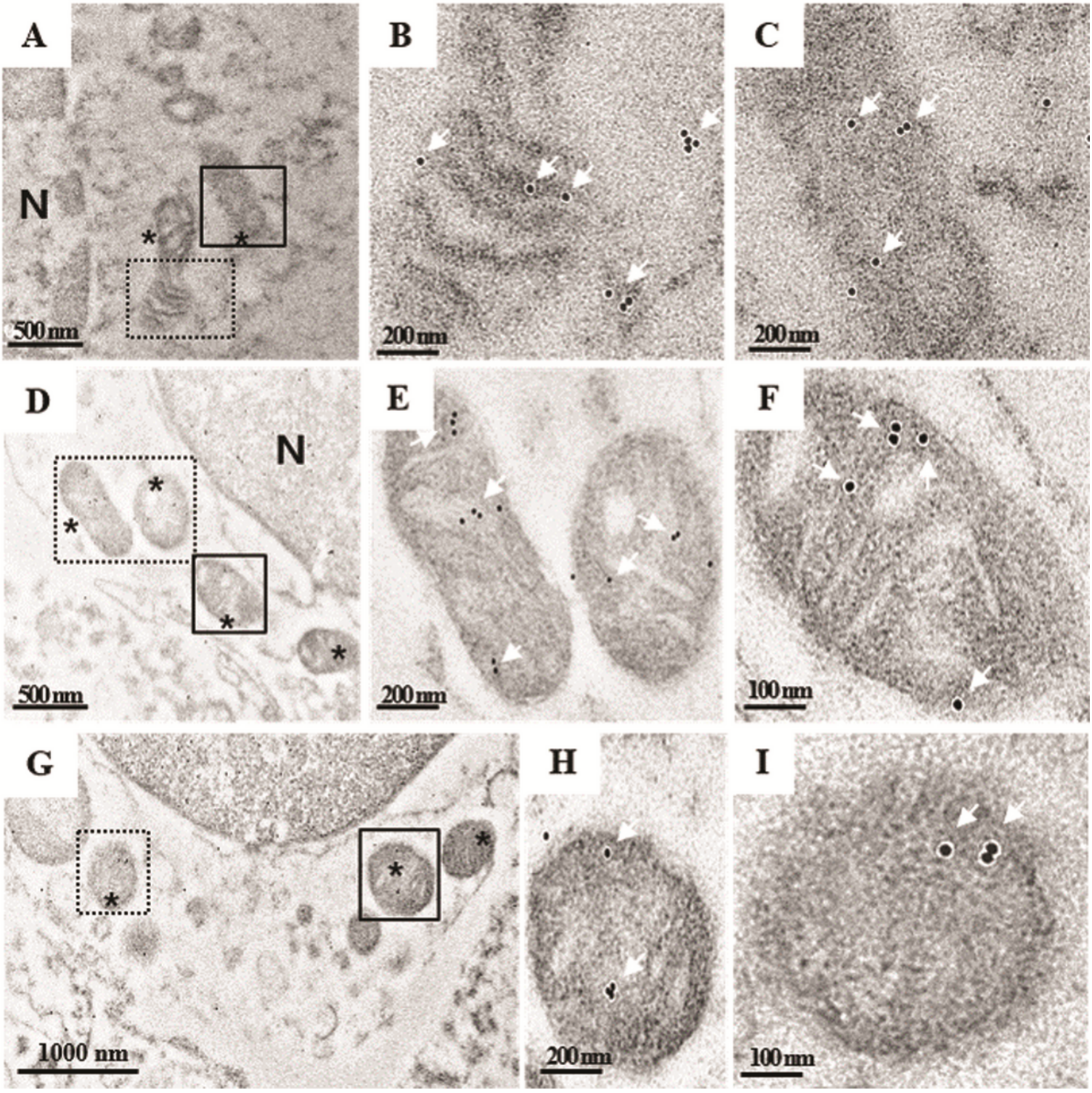


## Figure 4

Subcellular localization of DAPK1 in CSF cells from SAH patients with DCI. Expression and localization of DAPK1 were analyzed by immunogold labeling under EM. (A), (D), and (G) Damaged and swollen mitochondria with collapsed cristae are indicated with asterisks. Immunogold particles were mainly

detected in mitochondria (white arrows). (B-C), (E-F), and (H-I) Enlarged boxed areas in A, D and G, respectively.

## Supplementary Files

This is a list of supplementary files associated with this preprint. Click to download.

- SupplementalDataScireport.docx